A LETTERS JOURNAL EXPLORING THE FRONTIERS OF PHYSICS

February 2019

EPL, **125** (2019) 34003
doi: 10.1209/0295-5075/125/34003

www.epljournal.org

An acoustic imaging method for layered non-reciprocal media

KEES WAPENAAR and CHRISTIAN REINICKE

Department of Geoscience and Engineering, Delft University of Technology - Stevinweg 1, 2628 CN Delft, The Netherlands

received 3 October 2018; accepted in final form 6 February 2019
published online 8 March 2019

PACS 43.60.Pt – Signal processing techniques for acoustic inverse problems
PACS 43.35.Gk – Phonons in crystal lattices, quantum acoustics
PACS 43.60.Tj – Wave front reconstruction, acoustic time-reversal, and phase conjugation

Abstract – Given the increasing interest for non-reciprocal materials, we propose a novel acoustic imaging method for layered non-reciprocal media. The method we propose is a modification of the Marchenko imaging method, which handles multiple scattering between the layer interfaces in a data-driven way. We start by reviewing the basic equations for wave propagation in a non-reciprocal medium. Next, we discuss Green's functions, focusing functions, and their mutual relations, for a non-reciprocal horizontally layered medium. These relations form the basis for deriving the modified Marchenko method, which retrieves the wave field inside the non-reciprocal medium from reflection measurements at the boundary of the medium. With a numerical example we show that the proposed method is capable of imaging the layer interfaces at their correct positions, without artefacts caused by multiple scattering.

Introduction. – Currently there is an increasing interest for elastic wave propagation in non-reciprocal materials [1–5]. We propose a novel method that uses the single-sided reflection response of a layered non-reciprocal medium to form an image of its interior. Imaging of layered media is impeded by multiple scattering between the layer interfaces. Recent work, building on the Marchenko equation [6], has led to imaging methods that account for multiple scattering in 2D and 3D inhomogeneous media [7–10]. Here we modify Marchenko imaging for non-reciprocal media. We restrict ourselves to horizontally layered media, but the proposed method can be generalised to 2D and 3D inhomogeneous media in a similar way as has been done for reciprocal media in the aforementioned references.

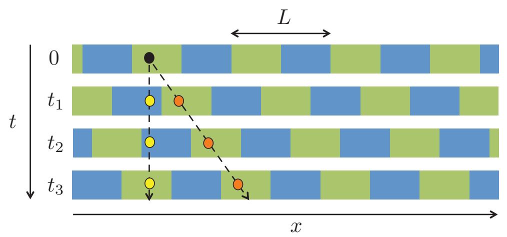

Fig. 1: A modulated 1D phononic crystal (adapted from Nassar *et al.* [4]). An observer at a fixed spatial position, indicated by the yellow dots, experiences a time-dependent medium, whereas an observer moving along with the modulating wave, indicated by the red dots, experiences a time-independent medium.

Wave equation for a non-reciprocal medium. – For simplicity, in this paper we approximate elastic wave propagation by an acoustic wave equation. Hence, we only consider compressional waves and ignore the conversion from compressional waves to shear waves and vice versa. This approximation is often used in reflection imaging methods and is acceptable as long as the propagation angles are moderate.

We review the basics of non-reciprocal acoustic wave propagation. For a more thorough discussion we refer to the citations given in the introduction. An example of a non-reciprocal material is a phononic crystal of which the parameters are modulated in a wave-like fashion [4]. Figure 1 shows a modulated 1D phononic crystal at a number of time instances. The different colours represent different values of a particular medium parameter, for example the compressibility κ. This parameter varies as a function of space and time, according to $\kappa(x,t) = \kappa(x - c_m t)$, where c_m is the modulation speed. The modulation wavelength is L. We define a moving coordinate $x' = x - c_m t$. The parameter κ in the moving coordinate system, $\kappa(x')$, is a function of space only. The same holds for the mass density $\rho(x')$. Acoustic wave propagation in a modulated material is analysed in a moving coordinate system, hence, in a time-independent medium. In this paper we assume the modulation speed is smaller than the lowest acoustic wave propagation velocity. Moreover, for the acoustic field we consider low frequencies, so that the wavelength of the acoustic wave is much larger than the modulation wavelength L. Using homogenisation theory, the small-scale parameters of the modulated material can be replaced by effective medium parameters. The theory for 3D elastic wave propagation in modulated materials, including the homogenisation procedure, is extensively discussed by Nassar *et al.* [4]. Here we present the main equations (some details are given in the supplementary material `Supplementarymaterial.pdf` (SM)). We consider a coordinate system $\mathbf{x} = (x_1, x_2, x_3)$ that moves along with the modulating wave (for notational convenience we dropped the primes). The x_3-axis is pointing downward. In this moving coordinate system the macroscopic acoustic deformation equation and equation of motion for a lossless non-reciprocal material read (leading-order terms only)

$$\kappa\partial_t p + (\partial_i + \xi_i\partial_t)v_i = 0, \tag{1}$$

$$(\partial_j + \xi_j\partial_t)p + \rho^o_{jk}\partial_t v_k = 0. \tag{2}$$

The operator ∂_t stands for temporal differentiation and ∂_i for differentiation in the x_i-direction. Latin subscripts (except t) take on the values 1 to 3. Einstein's summation convention applies to repeated Latin subscripts, except for subscript t. Field quantities $p = p(\mathbf{x}, t)$ and $v_i = v_i(\mathbf{x}, t)$ are the macroscopic acoustic pressure and particle velocity, respectively. Medium parameters $\kappa = \kappa(\mathbf{x})$ and $\rho^o_{jk} = \rho^o_{jk}(\mathbf{x})$ are the effective compressibility and mass density, respectively. Note that the effective mass density may be anisotropic, even when it is isotropic at the micro scale. It obeys the symmetry relation $\rho^o_{jk} = \rho^o_{kj}$. Parameter $\xi_i = \xi_i(\mathbf{x})$ is an effective coupling parameter.

We obtain the wave equation for the acoustic pressure p by eliminating the particle velocity v_i from eqs. (1) and (2). To this end, define ϑ_{ij} as the inverse of ρ^o_{jk}, hence, $\vartheta_{ij}\rho^o_{jk} = \delta_{ik}$, where δ_{ik} is the Kronecker delta function. Note that $\vartheta_{ij} = \vartheta_{ji}$. Apply ∂_t to eq. (1) and $(\partial_i + \xi_i\partial_t)\vartheta_{ij}$ to eq. (2) and subtract the results. This gives

$$(\partial_i + \xi_i\partial_t)\vartheta_{ij}(\partial_j + \xi_j\partial_t)p - \kappa\partial_t^2 p = 0. \tag{3}$$

As an illustration, we consider a homogeneous isotropic effective medium, with $\vartheta_{ij} = \delta_{ij}\rho^{-1}$. For this situation the wave equation simplifies to

$$(\partial_i + \xi_i\partial_t)(\partial_i + \xi_i\partial_t)p - \frac{1}{c^2}\partial_t^2 p = 0, \tag{4}$$

with $c = 1/\sqrt{\rho\kappa}$. Consider a plane wave $p(\mathbf{x}, t) = p(t - s_i x_i)$, with s_i being the slowness in the x_i-direction. Substituting this into eq. (4) we find the following relation for the slowness surface:

$$(s_1 - \xi_1)^2 + (s_2 - \xi_2)^2 + (s_3 - \xi_3)^2 = \frac{1}{c^2}, \tag{5}$$

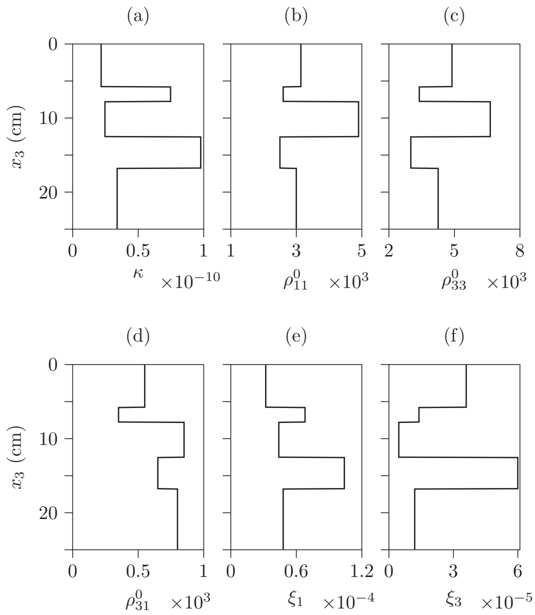

Fig. 2: Parameters of the non-reciprocal layered medium.

which describes a sphere with radius $1/c$ and its centre at (ξ_1, ξ_2, ξ_3). The asymmetry of this sphere with respect to the origin $(0, 0, 0)$ is a manifestation of the non-reciprocal properties of the medium.

Green's functions and focusing functions. – The Marchenko method, which we discuss in the next section, makes use of specific relations between Green's functions and focusing functions. Here we introduce these functions for a lossless non-reciprocal horizontally layered acoustic medium at the hand of a numerical example. Figure 2 shows the parameters of the layered medium as a function of the depth coordinate x_3. The half-space above the upper boundary $x_{3,0} = 0$ is homogeneous. For convenience we consider wave propagation in the (x_1, x_3)-plane (where x_1 and x_3 are moving coordinates, as discussed in the previous section). Hence, from here onward subscripts i, j and k in eqs. (1) and (2) take on the values 1 and 3 only.

For horizontally layered media it is convenient to decompose wave fields into plane waves and analyse wave propagation per plane-wave component. We define the plane-wave decomposition of a wave field quantity $u(x_1, x_3, t)$ as

$$u(s_1, x_3, \tau) = \int_{-\infty}^{\infty} u(x_1, x_3, \tau + s_1 x_1)\mathrm{d}x_1. \tag{6}$$

Here s_1 is the horizontal slowness and τ is a new time coordinate, usually called intercept time [11]. The relation with the more common plane-wave decomposition by Fourier transform becomes clear if we apply the temporal Fourier transform, $u(\omega) = \int_{-\infty}^{\infty} u(\tau)\exp(i\omega\tau)\mathrm{d}\tau$ to both sides of eq. (6), which gives

$$\tilde{u}(s_1, x_3, \omega) = \int_{-\infty}^{\infty} u(x_1, x_3, \omega)\exp(-i\omega s_1 x_1)\mathrm{d}x_1. \tag{7}$$

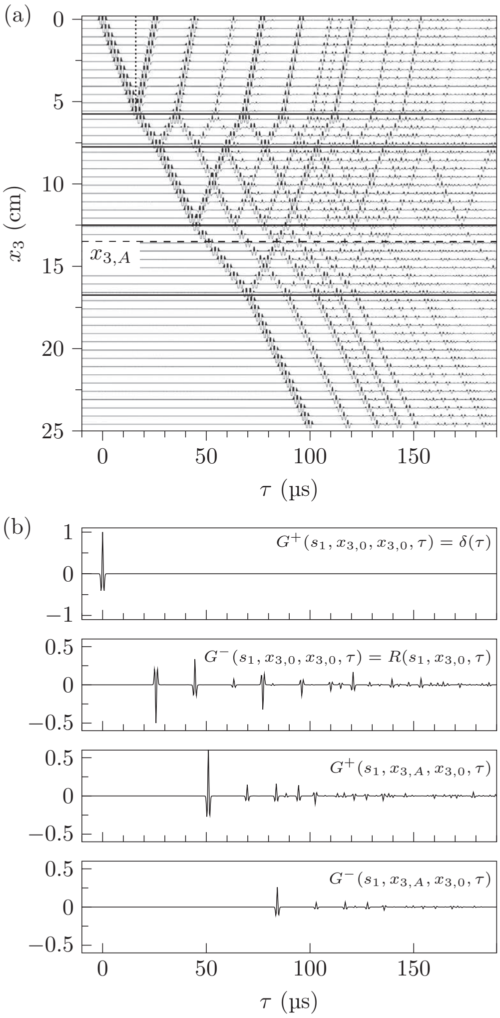

Fig. 3: (a) Green's function $G(s_1, x_3, x_{3,0}, \tau)$, for $s_1 = 0.22\,\mathrm{ms/m}$. (b) Decomposed Green's functions at $x_{3,0} = 0$ and $x_{3,A}$.

The tilde denotes the (s_1, x_3, ω)-domain The right-hand side of eq. (7) represents a spatial Fourier transform, with wave number $k_1 = \omega s_1$, where each wave number k_1 corresponds to a specific plane-wave component. Similarly, each horizontal slowness s_1 in eq. (6) refers to a plane-wave component.

Consider an impulsive downgoing plane wave, with horizontal slowness $s_1 = 0.22\,\mathrm{ms/m}$, which is incident to the layered medium at $x_{3,0} = 0$. We model its response, employing a (s_1, x_3, ω)-domain modelling method [12], adjusted for non-reciprocal media (based on eqs. (1) and (2), transformed to the (s_1, x_3, ω)-domain). The result, transformed back to the (s_1, x_3, τ)-domain, is shown in fig. 3(a) (for fixed s_1). Since it is the response to an impulsive source, we denote this field as a Green's function $G(s_1, x_3, x_{3,0}, \tau)$ (actually fig. 3(a) shows a band-limited version of the Green's function, in accordance with physical measurements, which are always band-limited). Note the different angles of the downgoing and upgoing waves directly left and right of the dotted vertical line in the first layer. This is a manifestation of the non-reciprocity of the medium. Figure 3(b) shows the decomposed fields at $x_{3,0} = 0$ and $x_{3,A}$, where $x_{3,A}$ denotes an arbitrary depth level inside the medium (taken in this example as $x_{3,A} = 13.5\,\mathrm{cm}$). The superscripts + and − stand for downgoing and upgoing, respectively. For the downgoing field at the upper boundary we have $G^+(s_1, x_{3,0}, x_{3,0}, \tau) = \delta(\tau)$, where $\delta(\tau)$ is the Dirac delta function. For the upgoing response at the upper boundary we write $G^-(s_1, x_{3,0}, x_{3,0}, \tau) = R(s_1, x_{3,0}, \tau)$, where $R(s_1, x_{3,0}, \tau)$ is the reflection response. This is the response one would obtain from a physical reflection experiment carried out at the upper boundary of the layered medium, translating it to the moving coordinate system and transforming it to the plane-wave domain, using eq. (6). The decomposed responses inside the medium, $G^\pm(s_1, x_{3,A}, x_{3,0}, \tau)$, which were obtained here by numerical modelling, are not available in a physical experiment. In the next section we discuss how these responses can be obtained from $R(s_1, x_{3,0}, \tau)$ using the Marchenko method. For this purpose, we introduce an auxiliary wave field, the so-called focusing function $f_1(s_1, x_3, x_{3,A}, \tau)$, which is illustrated in fig. 4(a). Here $x_{3,A}$ denotes the focal depth. The focusing function is defined in a truncated version of the medium, which is identical to the actual medium above $x_{3,A}$ and homogeneous below $x_{3,A}$. The four arrows at the top of fig. 4(a) indicate the four events of the focusing function leaving the surface $x_{3,0} = 0$ as downgoing waves; the arrow just below the dashed line indicates the focus. Figure 4(b) shows the decomposed focusing functions at $x_{3,0} = 0$ and $x_{3,A}$. The downgoing focusing function $f_1^+(s_1, x_{3,0}, x_{3,A}, \tau)$ at the upper boundary is designed such that, after propagation through the truncated medium, it focuses at $x_{3,A}$. The focusing condition at $x_{3,A}$ is $f_1^+(s_1, x_{3,A}, x_{3,A}, \tau) = \delta(\tau)$. The upgoing response at the upper boundary is $f_1^-(s_1, x_{3,0}, x_{3,A}, \tau)$. Because the half-space below the truncated medium is by definition homogeneous, there is no upgoing response at $x_{3,A}$, hence $f_1^-(s_1, x_{3,A}, x_{3,A}, \tau) = 0$. Note that the downgoing and upgoing parts of the focusing function at $x_{3,0}$ each contain 2^{n-1} pulses, where n is the number of interfaces in the truncated medium.

In a similar way as for reciprocal media [8,13], we derive relations between the decomposed Green's functions and focusing functions. For this we use general reciprocity theorems for decomposed wave fields $\tilde{u}^\pm(s_1, x_3, \omega)$ in two independent states A and B. These theorems read

$$\big(\tilde{u}_A^{+(\mathrm{c})}\tilde{u}_B^- - \tilde{u}_A^{-(\mathrm{c})}\tilde{u}_B^+\big)_{x_{3,0}} = \big(\tilde{u}_A^{+(\mathrm{c})}\tilde{u}_B^- - \tilde{u}_A^{-(\mathrm{c})}\tilde{u}_B^+\big)_{x_{3,A}} \quad (8)$$

and

$$\big(\tilde{u}_A^{+*}\tilde{u}_B^+ - \tilde{u}_A^{-*}\tilde{u}_B^-\big)_{x_{3,0}} = \big(\tilde{u}_A^{+*}\tilde{u}_B^+ - \tilde{u}_A^{-*}\tilde{u}_B^-\big)_{x_{3,A}}, \quad (9)$$

respectively, where superscript $*$ denotes complex conjugation. These theorems, but without the superscripts (c)

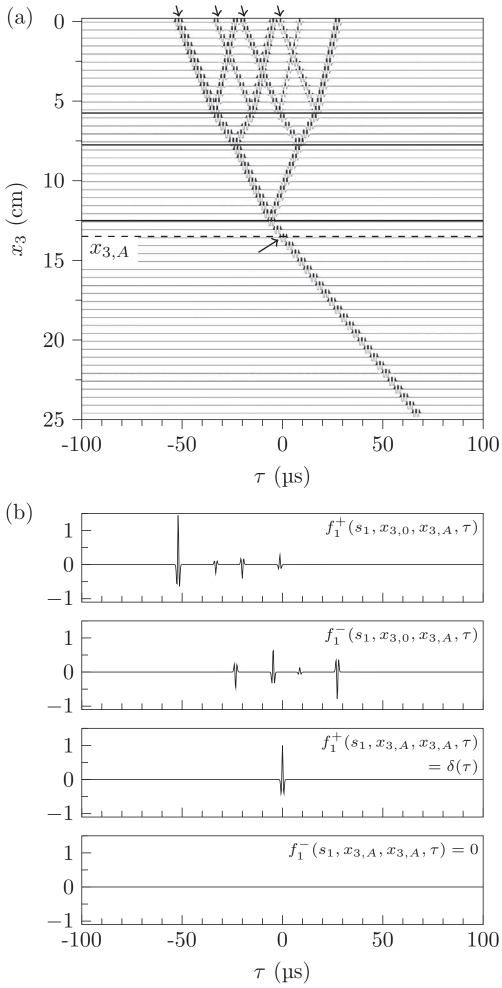

Fig. 4: (a) Focusing function $f_1(s_1, x_3, x_{3,A}, \tau)$, for $s_1 = 0.22\,\mathrm{ms/m}$. (b) Decomposed focusing functions at $x_{3,0} = 0$ and $x_{3,A}$.

in eq. (8), were previously derived for reciprocal media [14]. Whereas eq. (8) holds for propagating and evanescent waves, eq. (9) only holds for propagating waves. The extension to non-reciprocal media is derived in the SM. For non-reciprocal media, the superscript (c) at a wave field indicates that this field is defined in the complementary medium, in which the coupling parameter ξ_i, appearing in eqs. (1) and (2), is replaced by $-\xi_i$. The terminology "complementary medium" is adopted from the literature on non-reciprocal electromagnetic wave theory [15,16]. Note that, when wave fields with a tilde are written without their arguments (as in eqs. (8) and (9)), it is tacitly assumed that fields indicated by the superscript (c) are evaluated at $(-s_1, x_3, \omega)$.

To obtain relations between the decomposed Green's functions and focusing functions, we now take $\tilde{u}_A^\pm = \tilde{f}_1^\pm$ and $\tilde{u}_B^\pm = \tilde{G}^\pm$. The conditions at $x_{3,0}$ and $x_{3,A}$ discussed above are, in the (s_1, x_3, ω)-domain, $\tilde{G}^+(s_1, x_{3,0}, x_{3,0}, \omega) = 1$, $\tilde{G}^-(s_1, x_{3,0}, x_{3,0}, \omega) = \tilde{R}(s_1, x_{3,0}, \omega)$, $\tilde{f}_1^+(s_1, x_{3,A}, x_{3,A}, \omega) = 1$ and $\tilde{f}_1^-(s_1, x_{3,A}, x_{3,A}, \omega) = 0$. Making the appropriate substitutions in eqs. (8) and (9) we thus obtain

$$\tilde{G}^-(s_1, x_{3,A}, x_{3,0}, \omega) + \tilde{f}_1^{-(c)}(-s_1, x_{3,0}, x_{3,A}, \omega) = \tilde{R}(s_1, x_{3,0}, \omega)\tilde{f}_1^{+(c)}(-s_1, x_{3,0}, x_{3,A}, \omega) \tag{10}$$

and

$$\tilde{G}^+(s_1, x_{3,A}, x_{3,0}, \omega) - \{\tilde{f}_1^+(s_1, x_{3,0}, x_{3,A}, \omega)\}^* = -\tilde{R}(s_1, x_{3,0}, \omega)\{\tilde{f}_1^-(s_1, x_{3,0}, x_{3,A}, \omega)\}^*, \tag{11}$$

respectively. These representations express the wave field at $x_{3,A}$ inside the non-reciprocal medium in terms of reflection measurements at the surface $x_{3,0}$ of the medium. These expressions are similar to those in ref. [13], except that the focusing functions in eq. (10) are defined in the complementary medium. Therefore, we cannot follow the same procedure as in [13] to retrieve the focusing functions from eqs. (10) and (11). To resolve this issue, we derive a symmetry property of the reflection response $\tilde{R}(s_1, x_{3,0}, \omega)$ and use this to obtain a second set of representations. For the fields at $x_{3,0}$ in states A and B we choose $\tilde{u}_A^+ = \tilde{u}_B^+ = 1$ and $\tilde{u}_A^- = \tilde{u}_B^- = \tilde{R}$. Substituting this into the left-hand side of eq. (8) yields $\tilde{R}(s_1, x_{3,0}, \omega) - \tilde{R}^{(c)}(-s_1, x_{3,0}, \omega)$. We replace $x_{3,A}$ at the right-hand side of eq. (8) by $x_{3,M}$, which is chosen below all inhomogeneities of the medium, so that there are no upgoing waves at $x_{3,M}$. Hence, the right-hand side of eq. (8) is equal to 0. We thus find

$$\tilde{R}^{(c)}(-s_1, x_{3,0}, \omega) = \tilde{R}(s_1, x_{3,0}, \omega). \tag{12}$$

We obtain a second set of representations by replacing all quantities in eqs. (10) and (11) by the corresponding quantities in the complementary medium. Using eq. (12), this yields

$$\tilde{G}^{-(c)}(-s_1, x_{3,A}, x_{3,0}, \omega) + \tilde{f}_1^-(s_1, x_{3,0}, x_{3,A}, \omega) = \tilde{R}(s_1, x_{3,0}, \omega)\tilde{f}_1^+(s_1, x_{3,0}, x_{3,A}, \omega) \tag{13}$$

and

$$\tilde{G}^{+(c)}(-s_1, x_{3,A}, x_{3,0}, \omega) - \{\tilde{f}_1^{+(c)}(-s_1, x_{3,0}, x_{3,A}, \omega)\}^* = -\tilde{R}(s_1, x_{3,0}, \omega)\{\tilde{f}_1^{-(c)}(-s_1, x_{3,0}, x_{3,A}, \omega)\}^*, \tag{14}$$

respectively.

Marchenko method for non-reciprocal media. – In the previous section we obtained four representations, which we regroup into two sets. Equations (11) and (13) form the first set, containing only focusing functions in the truncated version of the actual medium. The second set is formed by eqs. (10) and (14), which contain only focusing functions in the truncated version of the complementary medium. All equations contain the reflection response $\tilde{R}(s_1, x_{3,0}, \omega)$ of the actual medium (*i.e.*, the measured data, transformed to the $(s_1, x_{3,0}, \omega)$-domain).

We now outline the procedure to retrieve the focusing functions and Green's functions from the reflection response, using the Marchenko method. The procedure is similar to that described in ref. [13]. For details we refer to this reference; here we emphasize the differences. The first set of equations (11) and (13), is transformed from the (s_1, x_3, ω)-domain to the (s_1, x_3, τ)-domain. Using time windows, the Green's functions are suppressed from these equations. Because one of the Green's functions is defined in the actual medium and the other in the complementary medium, two different time windows are needed, unlike in the Marchenko method for reciprocal media, which requires only one time window. Having suppressed the Green's functions, we are left with two equations for the two unknown focusing functions $f_1^+(s_1, x_{3,0}, x_{3,A}, \tau)$ and $f_1^-(s_1, x_{3,0}, x_{3,A}, \tau)$. These can be resolved from the reflection response $R(s_1, x_{3,0}, \tau)$ using the Marchenko method. This requires an initial estimate of the focusing function $f_1^+(s_1, x_{3,0}, x_{3,A}, \tau)$, which is defined as the inverse of the direct arrival of the transmission response of the truncated medium. In practice we define the initial estimate simply as $\delta(\tau + \tau_\mathrm{d})$, where $\tau_\mathrm{d} = \tau_\mathrm{d}(s_1, x_{3,0}, x_{3,A})$ is the travel time of the direct arrival, which can be derived from a background model of the medium. Since we only need a travel time, a smooth background model suffices; no information about the position and strength of the interfaces is needed. Once the focusing functions have been found, they can be substituted in the time domain versions of eqs. (11) and (13), which yields the Green's functions $G^+(s_1, x_{3,A}, x_{3,0}, \tau)$ and $G^{-(\mathrm{c})}(-s_1, x_{3,A}, x_{3,0}, \tau)$. Note that only the retrieved downgoing part of the Green's function, G^+, is defined in the actual medium. Therefore the procedure continues by applying the Marchenko method to the time domain versions of eqs. (10) and (14). This yields the focusing functions $f_1^{+(\mathrm{c})}(-s_1, x_{3,0}, x_{3,A}, \tau)$ and $f_1^{-(\mathrm{c})}(-s_1, x_{3,0}, x_{3,A}, \tau)$ and, subsequently, the Green's functions $G^{+(\mathrm{c})}(-s_1, x_{3,A}, x_{3,0}, \tau)$ and $G^-(s_1, x_{3,A}, x_{3,0}, \tau)$. Here the retrieved upgoing part of the Green's function, G^-, is defined in the actual medium. This completes the procedure for the retrieval of the downgoing and upgoing parts of the Green's functions in the actual medium at depth level $x_{3,A}$ for horizontal slowness s_1. This procedure can be repeated for any slowness corresponding to propagating waves and for any focal depth $x_{3,A}$.

Finally, we discuss how the retrieved Green's functions can be used for imaging. Similar as in a reciprocal medium, the relation between these Green's functions in the (s_1, x_3, ω)-domain is

$$\tilde{G}^-(s_1, x_{3,A}, x_{3,0}, \omega) = \tilde{R}(s_1, x_{3,A}, \omega)\tilde{G}^+(s_1, x_{3,A}, x_{3,0}, \omega), \tag{15}$$

where $\tilde{R}(s_1, x_{3,A}, \omega)$ is the plane-wave reflection response at depth level $x_{3,A}$ of the medium below $x_{3,A}$. Inverting this equation yields an estimate of the reflection response, according to

$$\langle \tilde{R}(s_1, x_{3,A}, \omega)\rangle = \frac{\tilde{G}^-(s_1, x_{3,A}, x_{3,0}, \omega)}{\tilde{G}^+(s_1, x_{3,A}, x_{3,0}, \omega)}. \tag{16}$$

Imaging the reflectivity at $x_{3,A}$ involves selecting the $\tau = 0$ component of the inverse Fourier transform of

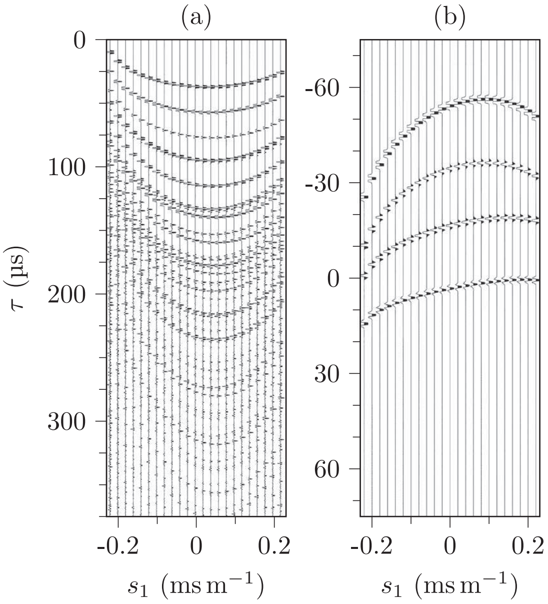

Fig. 5: (a) Modelled reflection response $R(s_1, x_{3,0}, \tau)$. (b) Retrieved focusing function $f_1^+(s_1, x_{3,0}, x_{3,A}, \tau)$.

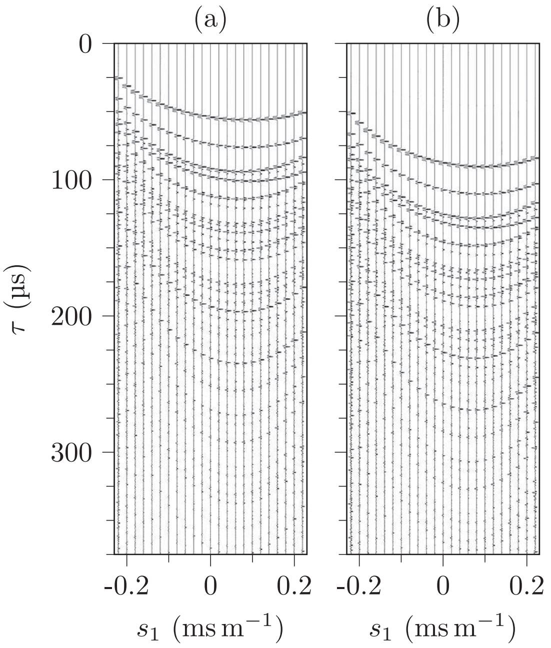

Fig. 6: (a) Retrieved Green's function $G^+(s_1, x_{3,A}, x_{3,0}, \tau)$. (b) Retrieved Green's function $G^-(s_1, x_{3,A}, x_{3,0}, \tau)$.

$\langle \tilde{R}(s_1, x_{3,A}, \omega)\rangle$, hence

$$\langle R(s_1, x_{3,A}, \tau = 0)\rangle = \frac{1}{2\pi}\int_{-\infty}^{\infty} \langle \tilde{R}(s_1, x_{3,A}, \omega)\rangle \mathrm{d}\omega. \tag{17}$$

Substituting eq. (16), stabilising the division (and suppressing the arguments of the Green's functions), we obtain

$$\langle R(s_1, x_{3,A}, 0)\rangle = \frac{1}{2\pi}\int_{-\infty}^{\infty} \frac{\tilde{G}^-\{\tilde{G}^+\}^*}{\tilde{G}^+\{\tilde{G}^+\}^* + \epsilon}\mathrm{d}\omega. \tag{18}$$

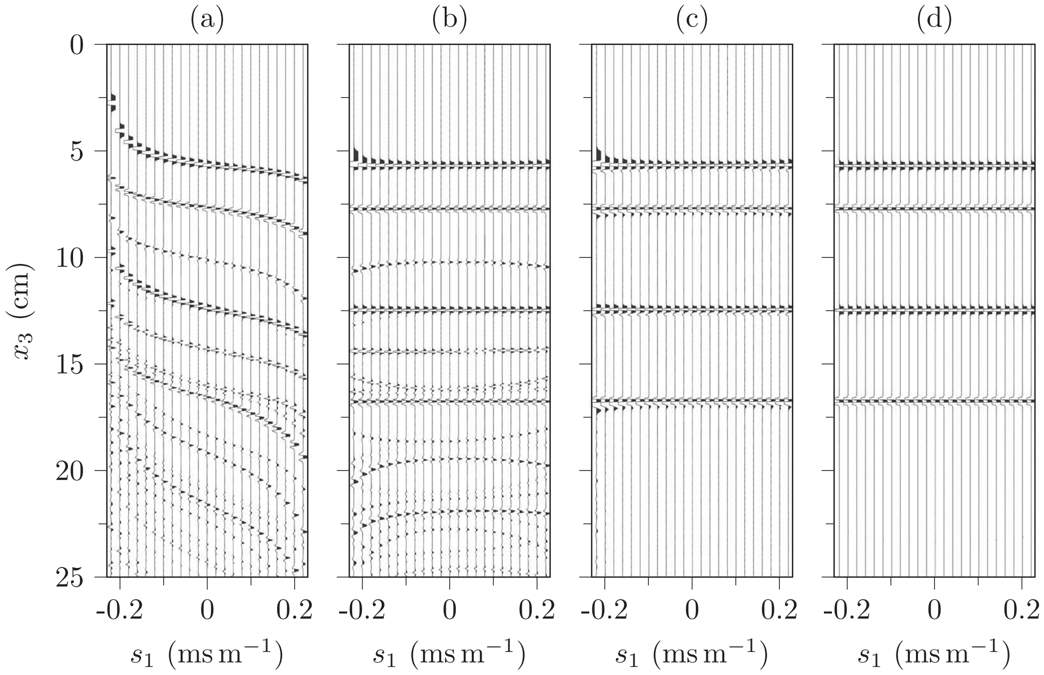

Fig. 7: Images of the layered non-reciprocal medium. (a) Primary image, accounting for anisotropy but ignoring non-reciprocity. (b) The same as panel (a) but accounting for non-reciprocity. (c) Marchenko image. (d) True reflectivity.

Numerical example. – We consider again the layered medium of fig. 2. Using the same modelling approach as before, we model the reflection responses to tilted downgoing plane waves at $x_{3,0} = 0$, this time for a range of horizontal slownesses s_1. The result, transformed to the $(s_1, x_{3,0}, \tau)$-domain and convolved with a wavelet with a central frequency of 600 kHz, is shown in fig. 5(a). To emphasize the multiples (only for the display), a time-dependent amplitude gain, using the function $\exp\{3\tau/375\,\mu\text{s}\}$, has been applied. Note the asymmetry with respect to $s_1 = 0$ as a result of the non-reciprocity of the medium. The last trace (for $s_1 = 0.22$ ms/m) corresponds with the second trace in fig. 3(b).

We define the focal depth in the fourth layer, at $x_{3,A} = 13.5$ cm. Using the Marchenko method, we retrieve the focusing functions $f_1^{\pm}(s_1, x_{3,0}, x_{3,A}, \tau)$ and $f_1^{\pm(c)}(-s_1, x_{3,0}, x_{3,A}, \tau)$ from the reflection response $R(s_1, x_{3,0}, \tau)$ and the travel times τ_d between $x_{3,0}$ and $x_{3,A}$. One of these focusing functions, $f_1^+(s_1, x_{3,0}, x_{3,A}, \tau)$, is shown in fig. 5(b). The last trace (for $s_1 = 0.22$ ms/m) corresponds with the first trace in fig. 4(b).

Using the reflection response and the retrieved focusing functions, we obtain the Green's functions $G^+(s_1, x_{3,A}, x_{3,0}, \tau)$ and $G^-(s_1, x_{3,A}, x_{3,0}, \tau)$ from the time domain versions of eqs. (11) and (10), see fig. 6 (same amplitude gain as in fig. 5(a)). From the Fourier transform of these Green's functions, an image is obtained at $x_{3,A}$ as a function of s_1, using eq. (18). Repeating this for all $x_{3,A}$ we obtain what we call the Marchenko image, shown in fig. 7(c). For comparison, fig. 7(a) shows an image obtained by a primary imaging method, ignoring the non-reciprocal aspects of the medium, and fig. 7(b) shows the improvement when non-reciprocity is taken into account (but multiples are still ignored). For comparison, fig. 7(d) shows the true reflectivity with the same filters applied as for the imaging results. Note that the match of the Marchenko imaging result with the true reflectivity is very accurate. The relative errors, except for the leftmost traces, are less than 2%.

Note that we assumed that the medium is lossless. In case of a medium with losses, modifications are required. For moderate losses that are approximately constant throughout the medium, one can apply a time-dependent loss compensation factor to the reflection response $R(s_1, x_{3,0}, \tau)$ before applying the Marchenko method (assuming an estimate of the loss parameter is available). Alternatively, when the medium is accessible from two sides, the Marchenko imaging method of Slob [17], modified for non-reciprocal media, can be applied directly to the data. This removes the need to apply a loss compensation factor.

Conclusions. – We have introduced a new imaging method for layered non-reciprocal materials. The proposed method is a modification of the Marchenko imaging method, which is capable of handling multiple scattering in a data-driven way (*i.e.*, no information is required about the layer interfaces that cause the multiple scattering). To account for the non-reciprocal properties of the medium, we derived two sets of representations for the Marchenko method, one set for the actual medium and one set for the complementary medium. Using a symmetry relation between the reflection responses of both media, we arrived at a method which retrieves all quantities needed for imaging (focusing functions and Green's functions in the actual and the complementary medium) from the reflection response of the actual medium. We illustrated the method with a numerical example, demonstrating the improvement over standard primary imaging methods. The proposed method can be extended for 2D and 3D inhomogeneous media, in a similar way as has been done for the Marchenko method in reciprocal media.

* * *

We thank an anonymous referee for a constructive review, which helped us to improve the readability of the paper. This work has received funding from the European Union's Horizon 2020 research and innovation programme: European Research Council (grant agreement 742703) and Marie Skłodowska-Curie (grant agreement 641943).

REFERENCES

[1] Willis J. R., *C. R. Mec.*, **340** (2012) 181.
[2] Norris A. N., Shuvalov A. L. and Kutsenko A. A., *Proc. R. Soc. A*, **468** (2012) 1629.
[3] Trainiti G. and Ruzzene M., *New J. Phys.*, **18** (2016) 083047.
[4] Nassar H., Xu X. C., Norris A. N. and Huang G. L., *J. Mech. Phys. Solids*, **101** (2017) 10.
[5] Attarzadeh M. A. and Nouh M., *J. Sound Vib.*, **422** (2018) 264.
[6] Marchenko V. A., *Dokl. Akad. Nauk SSSR*, **104** (1955) 695.
[7] Broggini F. and Snieder R., *Eur. J. Phys.*, **33** (2012) 593.
[8] Wapenaar K., Broggini F., Slob E. and Snieder R., *Phys. Rev. Lett.*, **110** (2013) 084301.
[9] van der Neut J. and Wapenaar K., *Geophysics*, **81** (2016) T265.
[10] Ravasi M., Vasconcelos I., Kritski A., Curtis A., da Costa Filho C. A. and Meles G. A., *Geophys. J. Int.*, **205** (2016) 99.
[11] Stoffa P. L., *Tau-p - A Plane Wave Approach to the Analysis of Seismic Data* (Kluwer Academic Publishers, Dordrecht) 1989.
[12] Kennett B. L. N. and Kerry N. J., *Geophys. J. R. Astron. Soc.*, **57** (1979) 557.
[13] Slob E., Wapenaar K., Broggini F. and Snieder R., *Geophysics*, **79** (2014) S63.
[14] Wapenaar C. P. A. and Grimbergen J. L. T., *Geophys. J. Int.*, **127** (1996) 169.
[15] Kong J. A., *Proc. IEEE*, **60** (1972) 1036.
[16] Lindell I. V., Sihvola A. H. and Suchy K., *J. Electromagn. Waves Appl.*, **9** (1995) 887.
[17] Slob E., *Phys. Rev. Lett.*, **116** (2016) 164301.

epl supplementary material

An acoustic imaging method for layered non-reciprocal media: Supplementary material

KEES WAPENAAR[1] and CHRISTIAN REINICKE[1]

[1] *Department of Geoscience and Engineering, Delft University of Technology, Stevinweg 1, 2628 CN Delft, The Netherlands*

PACS 43.60.Pt – Signal processing techniques for acoustic inverse problems
PACS 43.35.Gk – Phonons in crystal lattices, quantum acoustics
PACS 43.60.Tj – Wave front reconstruction, acoustic time-reversal, and phase conjugation

Abstract –We derive equations (1), (2), (8) and (9) in the main paper.

Acoustic wave equation for a non-reciprocal medium. – The theory for 3D elastic wave propagation in modulated materials, including the homogenisation procedure, is extensively discussed by Nassar et al. [1]. Here we discuss the main equations, simplified for the acoustic approximation. Consider a coordinate system $\mathbf{x} = (x_1, x_2, x_3)$ that moves along with the modulating wave. We start with the following two equations in the space-time $(\mathbf{x}, t)$ domain

$$\begin{aligned} \partial_t m_j &= -\partial_j p, && (1)\\ \partial_t \Theta &= \partial_i v_i. && (2) \end{aligned}$$

Operator ∂_t stands for temporal differentiation and ∂_i for differentiation in the x_i-direction. Latin subscripts (except t) taken the values 1 to 3. Einstein's summation convention applies to repeated Latin subscripts, except for subscript t. Equation (1) formulates equilibrium of momentum in the moving coordinate system (leading order terms only), where $m_j = m_j(\mathbf{x}, t)$ is the momentum density and $p = p(\mathbf{x}, t)$ the acoustic pressure. Equation (2) relates the cubic dilatation $\Theta = \Theta(\mathbf{x}, t)$ (leading order) to the particle velocity $v_i = v_i(\mathbf{x}, t)$. All field quantities in equations (1) and (2) are macroscopic quantities. The macroscopic constitutive equations are defined as

$$\begin{aligned} -p &= K\Theta + S_i^{(1)} v_i, && (3)\\ m_j &= S_j^{(2)}\Theta + \rho_{jk} v_k. && (4) \end{aligned}$$

Here $K = K(\mathbf{x})$ is the compression modulus, $\rho_{jk} = \rho_{jk}(\mathbf{x})$ the mass density, and $S_i^{(1)} = S_i^{(1)}(\mathbf{x})$ and $S_j^{(2)} = S_j^{(2)}(\mathbf{x})$ are coupling parameters. All these coefficients are effective parameters. Note that the effective mass density is anisotropic, even when it is isotropic at the micro scale. For a lossless non-reciprocal material, the medium parameters are real-valued and obey the following symmetry relations

$$\rho_{jk} = \rho_{kj} \quad \text{and} \quad S_j^{(2)} = -S_j^{(1)}. \tag{5}$$

We rewrite the constitutive equations (3) and (4) into explicit expressions for Θ and m_j, as follows

$$\begin{aligned} \Theta &= -\kappa p - \xi_i v_i, && (6)\\ m_j &= \xi_j p + \rho^o_{jk} v_k, && (7) \end{aligned}$$

where

$$\begin{aligned} \xi_i &= \kappa S_i^{(1)} && (8)\\ \rho^o_{jk} &= \rho_{jk} + \kappa S_j^{(1)} S_k^{(1)}, && (9)\\ \kappa &= 1/K, && (10) \end{aligned}$$

with $\rho^o_{jk} = \rho^o_{kj}$. Substitution of the modified constitutive equations (6) and (7) into equations (2) and (1) gives, after some reorganisation of terms,

$$\begin{aligned} \kappa\partial_t p + (\partial_i + \xi_i \partial_t) v_i &= 0, && (11)\\ (\partial_j + \xi_j \partial_t) p + \rho^o_{jk} \partial_t v_k &= 0. && (12) \end{aligned}$$

These are equations (1) and (2) in the main paper.

Matrix-vector wave equation. – From here onward we consider a horizontally layered medium, hence, we assume that the medium parameters are functions of the vertical coordinate x_3 only, i.e., $\kappa = \kappa(x_3)$, $\rho^o_{jk} = \rho^o_{jk}(x_3)$ and $\xi_i = \xi_i(x_3)$. For horizontally layered media it is convenient to decompose wave fields into plane waves and analyse wave propagation per plane-wave component. We define the Fourier transform from the space-time $(\mathbf{x}, t)$ domain to the slowness-space-frequency (s_α, x_3, ω) domain as

$$\tilde{u}(s_\alpha, x_3, \omega) = \int\int u(\mathbf{x}, t) \exp\{i\omega(t - s_\alpha x_\alpha)\} \mathrm{d}t \mathrm{d}x_\alpha, \quad (13)$$

where s_α denotes the horizontal slowness, ω the angular frequency and i the imaginary unit. Greek subscripts take on the values 1 and 2 and Einstein's summation convention applies to repeated Greek subscripts. Note that equation (13) accomplishes a decomposition into monochromatic plane waves.

We derive a matrix-vector wave equation of the following form

$$\partial_3 \tilde{\mathbf{q}} = \tilde{\boldsymbol{\mathcal{A}}} \tilde{\mathbf{q}}, \quad (14)$$

with wave vector $\tilde{\mathbf{q}} = \tilde{\mathbf{q}}(s_\alpha, x_3, \omega)$ defined as

$$\tilde{\mathbf{q}} = \begin{pmatrix} \tilde{p} \\ \tilde{v}_3 \end{pmatrix}. \quad (15)$$

Equation (14) is well-known for wave propagation in reciprocal media [2, 3]. For non-reciprocal media, matrix $\tilde{\boldsymbol{\mathcal{A}}}$ is obtained as follows. From equation (11) we extract an expression for $\partial_3 v_3$. We define ϑ_{ij} as the inverse of ρ^o_{jk}, hence, $\vartheta_{ij}\rho^o_{jk} = \delta_{ik}$, where δ_{ik} is the Kronecker delta function. Applying $\vartheta_{33}^{-1}\vartheta_{3j}$ to equation (12) yields an expression for $\partial_3 p$. By applying $\vartheta_{\alpha j}$ to equation (12) we obtain an expression for $\partial_t v_\alpha$. We use equation (13) to transform these three expressions to the slowness-frequency domain. In the transformed expressions, ∂_t is replaced by $-i\omega$ and ∂_α by $i\omega s_\alpha$ for $\alpha = 1, 2$. After elimination of $\tilde{v}_\alpha$ we thus obtain equation (14), with matrix $\tilde{\boldsymbol{\mathcal{A}}} = \tilde{\boldsymbol{\mathcal{A}}}(s_\alpha, x_3, \omega)$ defined as

$$\tilde{\boldsymbol{\mathcal{A}}} = \begin{pmatrix} i\omega\{\xi_3 - d_\alpha(s_\alpha - \xi_\alpha)\} & i\omega\vartheta_{33}^{-1} \\ i\omega\vartheta_{33}s_3^2 & i\omega\{\xi_3 - d_\alpha(s_\alpha - \xi_\alpha)\} \end{pmatrix}, \quad (16)$$

where

$$s_3^2 = \vartheta_{33}^{-1}\big(\kappa - (s_\alpha - \xi_\alpha)b_{\alpha\beta}(s_\beta - \xi_\beta)\big), \quad (17)$$

$$d_\alpha = \vartheta_{33}^{-1}\vartheta_{3\alpha}, \quad (18)$$

$$b_{\alpha\beta} = \vartheta_{\alpha\beta} - \vartheta_{\alpha 3}\vartheta_{33}^{-1}\vartheta_{3\beta}. \quad (19)$$

Decomposition. – We introduce a decomposed wave vector $\tilde{\mathbf{p}} = \tilde{\mathbf{p}}(s_\alpha, x_3, \omega)$ via

$$\tilde{\mathbf{q}} = \tilde{\boldsymbol{\mathcal{L}}} \tilde{\mathbf{p}}, \quad (20)$$

where

$$\tilde{\mathbf{p}} = \begin{pmatrix} \tilde{u}^+ \\ \tilde{u}^- \end{pmatrix}, \quad (21)$$

with $\tilde{u}^+$ and $\tilde{u}^-$ to be discussed later. We derive a wave equation for $\tilde{\mathbf{p}}$, following the same process as for reciprocal media [4, 5], modified for non-reciprocal media. The eigenvalue decomposition of matrix $\tilde{\boldsymbol{\mathcal{A}}}$ reads

$$\tilde{\boldsymbol{\mathcal{A}}} = \tilde{\boldsymbol{\mathcal{L}}}\tilde{\boldsymbol{\mathcal{H}}}\tilde{\boldsymbol{\mathcal{L}}}^{-1}, \quad (22)$$

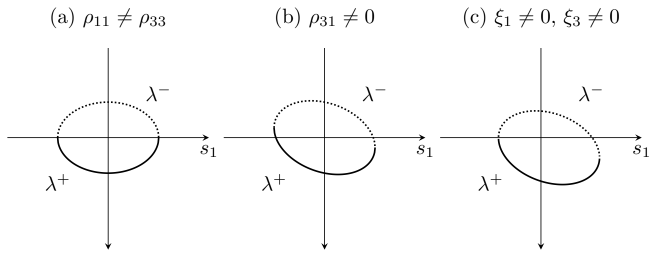

Fig. 1: Vertical slowness $\lambda^\pm$ as a function of horizontal slowness s_1 (and $s_2 = 0$). (a) Anisotropic reciprocal medium. (b) Idem, with tilted symmetry axis. (c) Idem, but for a non-reciprocal medium.

where

$$\tilde{\boldsymbol{\mathcal{H}}} = \begin{pmatrix} i\omega\lambda^+ & 0 \\ 0 & -i\omega\lambda^- \end{pmatrix}, \quad (23)$$

$$\tilde{\boldsymbol{\mathcal{L}}} = \frac{1}{\sqrt{2}}\begin{pmatrix} 1/\sqrt{\vartheta_{33}s_3} & 1/\sqrt{\vartheta_{33}s_3} \\ \sqrt{\vartheta_{33}s_3} & -\sqrt{\vartheta_{33}s_3} \end{pmatrix}, \quad (24)$$

$$\tilde{\boldsymbol{\mathcal{L}}}^{-1} = \frac{1}{\sqrt{2}}\begin{pmatrix} \sqrt{\vartheta_{33}s_3} & 1/\sqrt{\vartheta_{33}s_3} \\ \sqrt{\vartheta_{33}s_3} & -1/\sqrt{\vartheta_{33}s_3} \end{pmatrix}, \quad (25)$$

with

$$\lambda^\pm = s_3 \pm \{\xi_3 - d_\alpha(s_\alpha - \xi_\alpha)\}, \quad (26)$$

$$s_3 = \sqrt{\vartheta_{33}^{-1}\big(\kappa - (s_\alpha - \xi_\alpha)b_{\alpha\beta}(s_\beta - \xi_\beta)\big)}. \quad (27)$$

Substituting equations (20) and (22) into equation (14), we obtain

$$\partial_3 \tilde{\mathbf{p}} = \tilde{\boldsymbol{\mathcal{B}}} \tilde{\mathbf{p}}, \quad (28)$$

with

$$\tilde{\boldsymbol{\mathcal{B}}} = \tilde{\boldsymbol{\mathcal{H}}} - \tilde{\boldsymbol{\mathcal{L}}}^{-1}\partial_3\tilde{\boldsymbol{\mathcal{L}}}, \quad (29)$$

or, using equations (23) – (25),

$$\tilde{\boldsymbol{\mathcal{B}}} = \begin{pmatrix} i\omega\lambda^+ & -r \\ -r & -i\omega\lambda^- \end{pmatrix}, \quad (30)$$

with $\lambda^\pm$ defined in equations (26) and (27), and

$$r = -\frac{\partial_3(\vartheta_{33}s_3)}{2\vartheta_{33}s_3}. \quad (31)$$

Using equations (21) and (30), equation (28) can be written as

$$\partial_3\tilde{u}^+ = i\omega\lambda^+\tilde{u}^+ - r\tilde{u}^-, \quad (32)$$

$$\partial_3\tilde{u}^- = -i\omega\lambda^-\tilde{u}^- - r\tilde{u}^+. \quad (33)$$

Analogous to the reciprocal situation, this is a system of coupled one-way wave equations for downgoing waves $\tilde{u}^+$ and upgoing waves $\tilde{u}^-$, with λ^+ and λ^- representing the vertical slownesses for these waves, and r being the reflection function, which couples the downgoing waves to the upgoing waves and vice versa. Figure 1 is an illustration of the vertical slownesses.

Propagation invariants. – We consider two independent solutions $\tilde{\mathbf{p}}_A$ and $\tilde{\mathbf{p}}_B$ of wave equation (28) and show that specific combinations of these wave vectors (or "states") are invariant for propagation through the medium. Propagation invariants have been extensively used for wave fields in reciprocal media [6–9]. To derive propagation invariants for non-reciprocal media, we introduce a complementary medium, in which the coupling parameter ξ_i is replaced by $-\xi_i$ for $i = 1, 2, 3$. The wave vectors and matrices in a complementary medium are denoted by $\tilde{\mathbf{p}}^{(c)}$ and $\tilde{\boldsymbol{\mathcal{B}}}^{(c)}$, respectively. Using the definition of matrix $\tilde{\boldsymbol{\mathcal{B}}}$ in equation (30), with $\lambda^{\pm}$ defined in equations (26) and (27) and r in equation (31), it follows that $\tilde{\boldsymbol{\mathcal{B}}}$ obeys the following symmetry relations

$$\{\tilde{\boldsymbol{\mathcal{B}}}^{(c)}(-s_\alpha, x_3, \omega)\}^t\mathbf{N} = -\mathbf{N}\tilde{\boldsymbol{\mathcal{B}}}(s_\alpha, x_3, \omega), \quad (34)$$

$$\{\tilde{\boldsymbol{\mathcal{B}}}(s_\alpha, x_3, \omega)\}^\dagger\mathbf{J} = -\mathbf{J}\tilde{\boldsymbol{\mathcal{B}}}(s_\alpha, x_3, \omega), \quad (35)$$

where

$$\mathbf{N} = \begin{pmatrix} 0 & 1 \\ -1 & 0 \end{pmatrix}, \quad \mathbf{J} = \begin{pmatrix} 1 & 0 \\ 0 & -1 \end{pmatrix}. \quad (36)$$

Superscript t denotes transposition and $\dagger$ denotes transposition and complex conjugation. Equation (34) holds for all s_α, whereas equation (35) only holds for those s_α for which s_3 defined in equation (27) is real-valued, i.e., for $(s_\alpha - \xi_\alpha)b_{\alpha\beta}(s_\beta - \xi_\beta) \leq \kappa$. Real-valued s_3 corresponds to propagating waves, whereas imaginary-valued s_3 corresponds to evanescent waves. We consider the quantities $\partial_3(\{\tilde{\mathbf{p}}_A^{(c)}\}^t\mathbf{N}\tilde{\mathbf{p}}_B)$ and $\partial_3(\tilde{\mathbf{p}}_A^\dagger\mathbf{J}\tilde{\mathbf{p}}_B)$. When the arguments of functions are dropped, it is tacitly assumed that functions in the complementary medium, indicated by superscript (c), are evaluated at $(-s_\alpha, x_3, \omega)$. Applying the product rule for differentiation, using equation (28) and symmetry relations (34) and (35), we find

$$\partial_3(\{\tilde{\mathbf{p}}_A^{(c)}\}^t\mathbf{N}\tilde{\mathbf{p}}_B) = 0 \quad (37)$$

and

$$\partial_3(\tilde{\mathbf{p}}_A^\dagger\mathbf{J}\tilde{\mathbf{p}}_B) = 0. \quad (38)$$

From these equations it follows that $\{\tilde{\mathbf{p}}_A^{(c)}\}^t\mathbf{N}\tilde{\mathbf{p}}_B$ and $\tilde{\mathbf{p}}_A^\dagger\mathbf{J}\tilde{\mathbf{p}}_B$ are independent of x_3 (the latter only for propagating waves). These quantities are therefore called propagation invariants.

Reciprocity theorems. – Using the definitions of $\tilde{\mathbf{p}}$, $\mathbf{N}$ and $\mathbf{J}$ in equations (21) and (36), equations (37) and (38) imply

$$\big(\tilde{u}_A^{+(c)}\tilde{u}_B^- - \tilde{u}_A^{-(c)}\tilde{u}_B^+\big)_{x_{3,0}} = \big(\tilde{u}_A^{+(c)}\tilde{u}_B^- - \tilde{u}_A^{-(c)}\tilde{u}_B^+\big)_{x_{3,A}} \quad (39)$$

and

$$\big(\tilde{u}_A^{+*}\tilde{u}_B^+ - \tilde{u}_A^{-*}\tilde{u}_B^-\big)_{x_{3,0}} = \big(\tilde{u}_A^{+*}\tilde{u}_B^+ - \tilde{u}_A^{-*}\tilde{u}_B^-\big)_{x_{3,A}}, \quad (40)$$

respectively, where superscript $*$ denotes complex conjugation and $x_{3,0}$ and $x_{3,A}$ denote two depth levels. These are the reciprocity theorems of equations (8) and (9) in the main paper.

REFERENCES

[1] Nassar H., Xu X. C., Norris A. N. and Huang G. L., *Journal of the Mechanics and Physics of Solids*, **101** (2017) 10.

[2] Gilbert F. and Backus G. E., *Geophysics*, **31** (1966) 326.

[3] Frasier C. W., *Geophysics*, **35** (1970) 197.

[4] Kennett B. L. N. and Kerry N. J., *Geophysical Journal of the Royal Astronomical Society*, **57** (1979) 557.

[5] Kennett B. L. N. and Illingworth M. R., *Geophysical Journal of the Royal Astronomical Society*, **66** (1981) 633.

[6] Haines A. J., *Geophysical Journal International*, **95** (1988) 237.

[7] Kennett B. L. N., Koketsu K. and Haines A. J., *Geophysical Journal International*, **103** (1990) 95.

[8] Koketsu K., Kennett B. L. N. and Takenaka H., *Geophysical Journal International*, **105** (1991) 119.

[9] Takenaka H., Kennett B. L. N. and Koketsu K., *Wave Motion*, **17** (1993) 299.